Fracture Analysis of Beam-Column Joints due to Bond-Slip Mechanism

D. Jankovic
Delft University of Technology, Civil Engineering and Geo-Sciences Dep., Delft, The Netherlands

M. B. Chopra
University of Central Florida, Department of Civil and Environmental Engineering, Orlando, USA

S. K. Kunnath
University of California at Davis, Department of Civil and Environmental Engineering, Davis, USA

ABSTRACT: In order to predict a bond-slip behavior of the reinforcement bar in inner joint in a 'seismic' reinforced concrete frame structure, experiments and numerical analyses were conducted. A reinforced cylinder with a centrally embedded deformed rebar served as a simple joint model. The bar was fully loaded on a protruding end. Cyclic loading was applied neither in the experiments nor in the numerical analysis since the first intention was to numerically simulate the experiments. Bond-slip mechanism was studied as an axisymmetrical 2-D problem using DIANA Finite Element Analysis. The input data for the numerical analysis were used from the previously conducted experiments. The influence of the variations in the bar embedment length (full/local) as well as the addition of a different percentage of polypropylene fibers in fiber reinforced concrete on bond-slip, bond stress, deformation and cracking patterns was examined. The results from the numerical analysis are presented.

1 INTRODUCTION

The design of inner joints in a reinforced concrete frame structure under the seismic load points to a problem of proper force transmission through the joints since large shear forces develop in beam-column joints (Paulay et al. 1978). Bars, that go through the interior joints, are exposed to 'pushing' and 'pulling' of the adjacent beams in order to transfer the force from steel to the surrounding concrete. Shear force is transmitted in the interface zone between concrete and steel by bond stresses, which can be extremely large and exceed material bond strength.

Once a bar is loaded the strain in the interface between the concrete and steel in the joint does not remain constant over a bar length. The difference in the strain in concrete and steel interface invokes the mechanism of bond slipping (Lutz & Gergely 1967) due to the insufficient bond capacity. A 'development length' (the accepted term from ACI rather than a bond stress) in the interior joint for a given size of a straight beam bar is usually larger than the depth of the adjacent column but also insufficient to form an adequate bond capacity. Depending on the size of the development length (shortest bar length in which steel stress increases to the yield strength f_y), steel yielding or concrete cracking may appear.

A slipping might be allowed to some extend in the frame joints where no seismic load was expected (Mindess 1989). However, the reinforced concrete frame structures in the seismic zones are designed to be ductile in order to resist seismic forces. Bond stresses that exceed the bond strength, developed at the bar-concrete interface, could result in bond-slip and significantly influence the hysteretic response of ductile frames. A 15% loss in bond strength may cause a loss of about 30% of the energy dissipation capacity in a typical beam-column joint (Pauley & Priestley 1992).

1.1 *How to improve bond strength?*

Much effort in the past has been devoted to the improvement of the bond characteristics in the interface zone between bar and concrete using deformed instead of plain bars (Abrams 1913) in order to resist slipping with a mechanical interlock. The succeeding research concentrated mostly on the deformed reinforcement re-modeling taking into account different shapes of ribs and rib face angle, height of ribs, rib-spacing etc. (Brown et al. 1993, Goto 1971, Lutz & Gergely 1967, Clark 1946, 1949). Less has been done on the improvement of the bond strength of concrete although shear- and bond strength are affected by the tensile strength of concrete. The tensile strength develops more quickly than the compressive strength and influences quick development of shear- and bond strength (MacGregor 1997). Although the first cracks appear in the interface zone, most likely due to the break of concrete compression strength, the concrete core collapses due to the con-

crete splitting. ACI Committee 544 (1982, 1994) recommended the usage of fiber reinforced concrete (FRC) for seismic resistance to increase the concrete tensile strength.

Regarding compressive strength, Yin et al. (1989, 1990) presented the results of different compression tests (uniaxial and biaxial test) with plain concrete and FRC. The FRC compression strength increased by as much as 35% in biaxial tests while only a few insignificant percent in uniaxial compression. Studies by Soroushian et al. (1994) proved that bond strength increased with the fiber addition.

Following the recommendations from ACI-ASCE Committee 352 (1976) as well as ACI Committee 544 (1982) for the improvement of design for seismic joints, experimental and numerical research was undertaken. The experiments (Moradi 1994) have been performed in order to observe bond-slip in seismic joints and its influence to the concrete behavior. A concrete cylinder, made of ordinary and fiber reinforced concrete, centrally reinforced with a single embedded deformed bar, modeled the inner joint of the reinforced concrete frame. In the fiber reinforced concrete, the polypropylene fibers of two fiber lengths: 'short' length 19 mm (0.75 in.) and 'long' length of 50 mm (2 in.) were added to the cement matrix. During the experiments, only mixes with fibers in 0.5% and 1% per volume were used due to the mix unworkablility and bundling of fibers when a higher fiber percentage was added.

A deformed steel bar ϕ22 (# 7, Grade 60, nominal strength f_y = 414 MPa) was embedded in the concrete cylinders at different embedment lengths (Moradi 1994, Jankovic 1998). The bar had laterallugs and the total bar length was 300 mm (12 in.). The diameter ratio of the cylinder 300 mm x 250 mm (12 in. x 10 in.) to the rebar ϕ22 was approximately 11. The bar embedment length in some samples was 150 mm (6 in.), so-called full embedment, out of total 300 mm (12 in). Other samples had a shorten development length (local embeddment length) of 50 mm (2 in.) and 75 mm (3 in.). The local bond was provided by two 50 mm PVC tubing around the rebar (Moradi 1994) which were sealed at the ends with grout to prevent penetration of concrete into the tubing. The reason for using the local and full embedment was to investigate the influence of the development length on the bond-slip.

The inverted cylindrical specimens were mounted in a Universal Testing machine so that pull-out forces could be applied at one end of the reinforcing bar (Moradi 1994). Load measurements were obtained through direct readings from the machine's pressure transducer while deformations were computed from a precision gage mounted to a fixed location in the bar.

2 FINITE ELEMENT ANALYSIS

The numerical analysis was first verified consulting the simulation of the pull-out tests by Gijsbers et al. (1978). In the current numerical analysis, half of the cylinder from the experiments was considered (Fig. 1) due to the axial symmetry (Jankovic 1998). Linear 2-D analysis was followed by the non-linear fracture analysis in DIANA finite element program (ver. 6.2, 1996) applying the available data from the experiments. Numerical load-tests were performed as an incremental displacement control tests, applied at the end of the rebar.

2.1 *Finite element mesh and material modeling*

Concrete was modeled by eight nodded quadratic iso parametric elements solid ring (100 elements); six truss three-nodded curved elements were used for the modeling of a deformed bar. The nonlinearity was introduced in the interface concrete-steel zone, with the six nodes line interface (bond) elements. These elements were skipped in the bar length of about 50 mm where bar enters the concrete and where no bond was expected (Gijsbers et al. 1978). The line interface elements modeled the relationship between debonding and slipping behavior (displacement in x and y direction) and bond stress (tractions in the tangential direction t_t and the radial direction t_n). For that purpose, dual nodes at the concrete-steel interface were applied. In order to calibrate the FEM model to match with the experimental results, the shear and normal stiffness of the interface (bond) elements varied between 100 and 300 N/mm^3. The chosen stiffness value was assumed and kept constant throughout the linear and the nonlinear analysis due to the DIANA programming limitations on PC. The value for the maximum bond stress was accepted as 5 N/mm^2 in the linear zone (Gijsbers et al. 1978, De Groot et al. 1981).

For the reinforcement, an elastic-plastic model, both in tension and compression, was used applying Von Mises criterion.

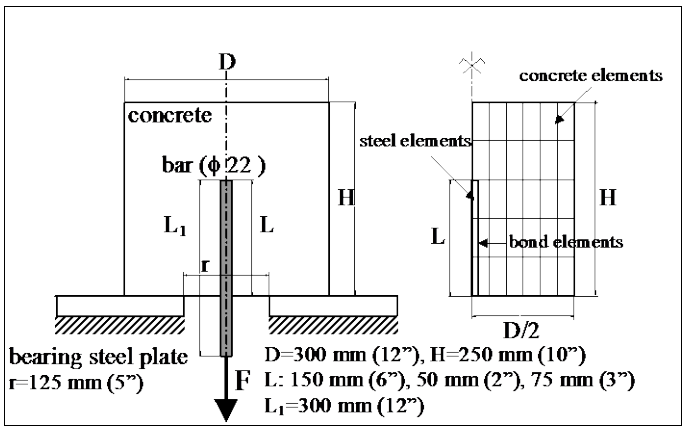

Figure 1. The model of a cylinder and schematic drawing of the element mesh used in the numerical analysis.

In general, concrete has been numerically modeled by using two different models based upon its behavior under tension and compression: a crack model valid for the load combinations with at least one tensile component involved and a plasticity model for describing the concrete behavior under multiaxial compressive stress. The concrete was modeled as a linear material before cracks occurred. The Young's modulus (E) and the Poisson's ratio (ν) were specified and assumed to have constant values throughout the analyses. For concrete in compression, an elastic-plastic model has been chosen. Calculated E value for the plain concrete varied from 19786 MPa to 23223 MPa (2869 ksi to 3367 ksi) but was lowered to 10000 MPa (Gijsbers et al. 1978). A multiaxial state of stress was applied. For concrete as a brittle material the Mohr-Coulomb yield criterion (in 2-D) was selected as well as Mohr-Coulomb friction model. It was assumed that the shear stress τ on the fracture plane was induced by friction.

In the analysis of FRC specimens, the Young's modulus (E) and Poisson's ratio (ν) depended on the additional percentage of fibers in 0.5% and 1% (ACI Committee 544 1982, 1994). The Young's modulus was increased to 30000 MPa with Poisson's ratio of 0.4. Regarding Coulomb failure criterion, Nielsen et al. (1978) suggested that a rigid-plastic constitutive model was assumed for the FRC with zero tensile cut-off. The same procedure was attempted in the numerical analysis but the results had not been as expected. The value for tensile cut-off was calculated as a fraction of the compression strength, which was assumed to be the same as in the case of plain concrete. Yield criterion for concrete was kept as Mohr-Coulomb with cohesion. The value for the friction angle was decreased from 55° to 30°.

2.2 *Fracture analysis*

The crack model based on strength criterion was used for a crack initiation. The fracture mechanics approach implemented in DIANA through material modelling was applied for the crack propagation. The application of fracture mechanics to concrete structures has been discussed for many years due to the heterogeneity and non-linearity of concrete. It was inappropriate to apply linear fracture mechanics (LEFM) to concrete (LEFM being a theory only valid for linear-elastic and macroscopic homogeneous materials).

In the case of bond-slipping, due to the brittleness and splitting nature of concrete (loss of bond results from the concrete splitting nature, Brown et al. 1993), fracture mechanics can be applied. According to Tepfers (1979), Reinhardt & van der Veen (1992) compressive forces develop due to the bar pull-out and grow to the circumferential forces forming a hydrostatic pressure on the inner ring part. Cracked inner concrete part has a conical shape while the rest of the concrete stays elastic. Cracks develop at the very early load period, long before the maximum pull-out force is reached.

Since cracking in heterogeneous material such as concrete is a very complex phenomenon, fracture process mechanisms can be quantified by distribution of energy during the fracture process (Shah 1995). Energy criteria can be used for crack propagation. Fracture energy release rate G_f (Griffith 1921) is used as a fracture parameter and a material property and the criterion for the crack propagation. In fracture mechanics theory, combination of two criteria, yield and fracture criterion gives the best way to find a safe region in the material.

RILEM (1985) established a method for the experimental determination of G_f as the energy required for breaking a notched three-point bend specimen into two pieces. When a crack starts to propagate, the amount of stored energy is released. The energy criterion states that the crack propagates when the released energy is equal or greater than the absorbed energy.

In plain concrete, the fracture energy G_f was 0.09 Nmm/mm^2 (90.5 J/m^2) with linear softening. This value was obtained by the curve fitting (Wittmann et al. 1987, 1988). RILEM (1985) suggested a higher value of 0.112 Nmm/mm^2 (112.5 J/m^2). For FRC, G_f was increased to 0.15 Nmm/mm^2 (150 J/m^2) with linear and exponential softening. Mode I and mode II were both included in the non-linear analysis since both opening and sliding mode contribute to the shear failure.

Cracking in concrete was modeled combining a tension cut-off, tension softening and shear retention. Tension cut-off has been taken as linear i.e. crack arises if the major principal tensile stress exceeds the value for f_t and $f_t(1+\sigma_{lateral}/f_c)$ where $\sigma_{lateral}$ is the lateral principal stress. The important parameter related to the concrete cracking is the shear retention factor β which takes into account a reduction of the shear stress that is transferred through the cracked concrete and it also models aggregate interlock. The β value is based on the experience and it varies in the range $0<\beta<1$ (Reinhardt 1989). The value for β has been taken as $\beta=0.2$ as it leads to similar results compared to the most of the experiments. This showed that the influence of β value was significant in a way that the inclination of the diagonal crack decreased with decreasing the β value. In the present study, β value was kept constant.

3 EFFECT OF FIBER CONTENT AND EMBEDMENT LENGTH

The effect of fiber content on the load capacity, bond stress and crack pattern was investigated for the cases of plain concrete and FRC cylinders. The fibers of 19 mm (0.75 in.) 'short' and 50 mm (2 in.)

'long' were added to the plain concrete in 0.5% and 1% by volume. The embedment lengths varied from: the 'full' bond length 150 mm (6 in.) to the local 50 (2 in.) and 75 mm (3 in.).

3.1 *Full embedment length*

The reinforcement 'full' embedment length in the cylindrical specimens of 300 mm x 250 mm (12 in. x 10 in.) was kept constant 150 mm (6 in.), in the first tests group. In this test-group (1A, 6B, 3C), only the percentage of fibers (0%, 0.5% and 1%) has been varied.

Experimental and numerical results were compared (Fig. 2). Both results confirmed an increase in force and bond stress when the fiber percentage was increased. Linear concrete behavior was assumed before cracks occurred and softening behavior after the peak load. The peak load increase in the specimens 3C (1% fibers) was more emphasized in the numerical analysis (Fig. 2a) than in the experiments due to the parameters approximation. Numerical results gave the minimum peak load value (96 kN) for the samples without fibers. The maximum reached 125 kN (30% increase) with 1% of fiber addition. The experimental maximum peak load was 102 kN for 1% of fibers and 82 kN (20% less) for plain concrete samples (Fig. 2b). The results did not show

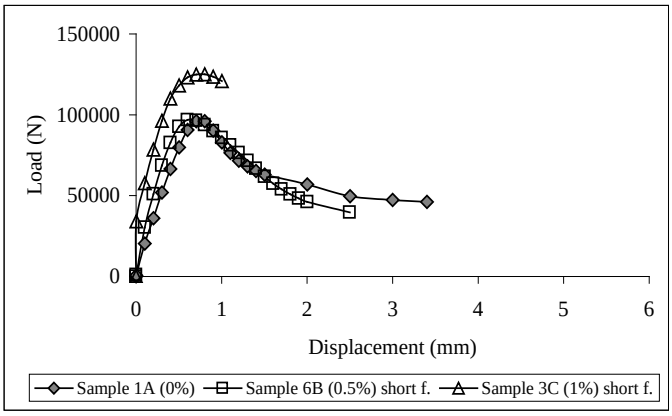

(a)

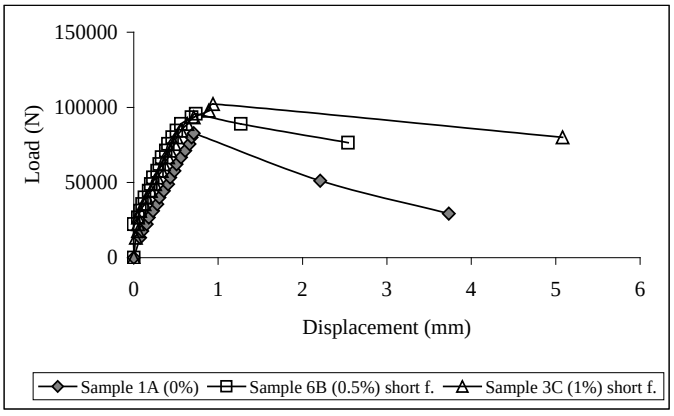

(b)

Figure 2. The effect of different fiber content in (a) FEM analysis and (b) experimental results with the embedment length of 150 mm (6 in.).

considerable variations in the peak load with the increase of fiber volume from 0% to 1%.

The experimental bond stress was the highest for 1% with 9.6 MPa. The bond stress for 0% and 0.5% was decreased for 17%. The maximum bond stress in the FEM was 17.6 MPa (1% fibers). The stress value was lower for about 20% in plain concrete and FRC with 0.5% fibers. Almost the same displacement values occurred both in the numerical analysis and in the experiments. The increase in the fiber content has not influenced the displacements. All peak displacement values varied in the range from 0.6 to 0.8 mm. In the case of numerical specimen model with 1% fibers the maximum displacement was not longer than 1 mm since the results did not converge any more. The difference in the experimental and numerical results might occurred due to the difference in the assumed Young's modulus since the computed results gave always stiffer behavior than the observed results in the experiments.

3.2 *Local bond length*

The load-displacement curves for the cases with the full and the local bond are introduced in Figures 3-4. The samples with no fiber addition (Fig. 3a) showed the regular load increase for 14% with the increase of the embedment length from 50 mm (71 kN) to 150 mm (83 kN). The FEM displacements at peak values were more or less the same for all bond lengths and varied from 0.7 mm to 0.8 mm. Bond stress had the opposite value: the maximum (20 MPa) was achieved with 50 mm embedment. The lowest stress was 13.5 MPa in the case of 150 mm (6 in.). Comparisons with the experiments (Fig. 3b) showed the load increase of 13% with 150 mm (6 in.) embedment length. The minimum force was measured with the bond length of 50 mm (2 in.), which is 38% less than calculated. The displacements, at which these peak values were reached, increased with the increase in bond length. The maximum bond stress was 11 MPa for 50 mm (2 in.) and the minimum was 7.8 MPa.

In the Figure 4 all samples had the same fiber content (0.5%) and different embedment. An increase in the load is observed with the increase of the embedment length (Fig. 4a). The maximum load 97 kN was reached with 150 mm (6 in.) in the Figure 4a (higher than in the Figure 3a) and the minimum was 64 kN for 50 mm (2 in.), less than without fibers. The analysis convergence for the sample 3D stopped at 2.1 mm slippage. After the peak has been reached, the bearing of the load became the same for all three samples. Bond stress showed rather different values for local and full embedment length. The highest value was 18.2 MPa for the bond of 50 mm (2 in.) embedment. It decreased to 15.1 MPa with 75 mm (3 in.). For the full embedment of 150 mm (6 in.), the bond stress value was 13.2 MPa.

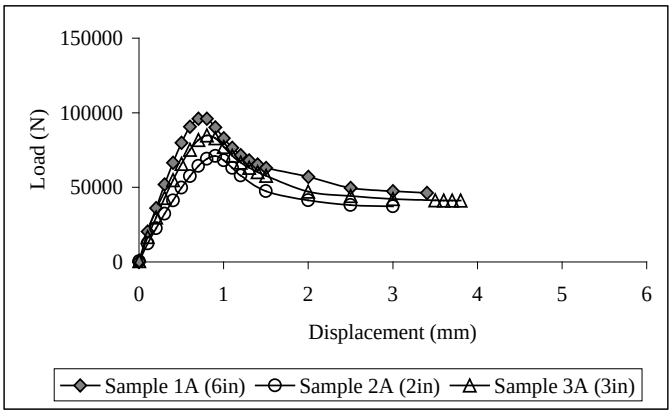

(a)

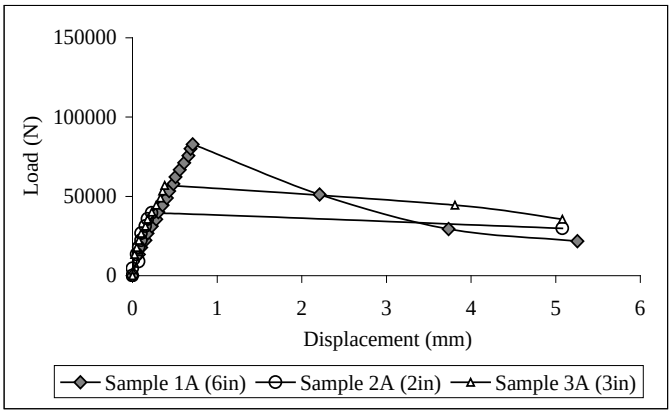

(b)

Figure 3. Load vs. displacement in the samples with no fiber addition, comparison of full and local embedment length (a) FEM results and (b) experimental results.

A similar trend has been seen in the experiments (Fig. 4b). The displacement at the maximum peak load differed showing rather scattered values of Young's modulus . Again, the maximum load was reached for 150 mm (6 in.) embedment as 97 kN. The lowest force was for 50 mm (53 kN). Regarding the bond stress, the highest value was 16 MPa for 75 mm and 14.7 MPa for 50 mm.

3.3 *Bond stress distribution*

With respect to the interface elements in the FEM model, the bond stress distribution for both components, radial and shear, was calculated. Shear bond stress is presented in Figure 5 along the specimen without/with fibers. When the full embedment length was shorten to the local, the stress distribution had two concentration peaks at the nodes where no-bond zone ended (Fig. 5). The difference of only 25 mm (1 in.) in local bond samples gave a visible difference in the values of shear stress in the case of no fiber addition (Fig. 5a). In the case of full embedment length (150 mm), the stress was distributed more evenly along the specimen length. Bond stress did not show any change in sign like in case of the pull-out test when the force was applied on both sides of the specimen (Gijsbers et al. 1978). A comparison of the shear stress between 0% and 0.5%

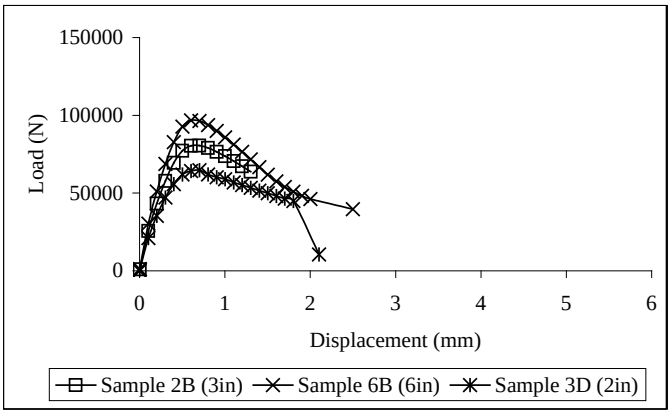

(a)

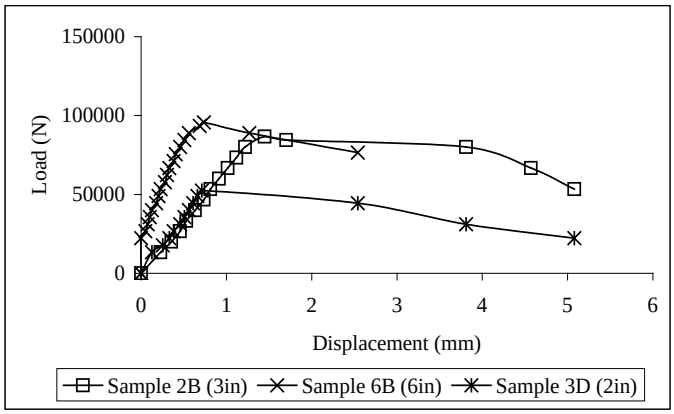

(b)

Figure 4. Load vs. displacement in FRC (0.5% fibers) samples with the full (150 mm) and local 50 mm (2 in.) and 75 mm (3 in.) embedment length in (a) FEM results and (b) experiments.

fiber addition with 150 mm (6 in.) embedment length, showed an increase in the shear stress for the max of 10 MPa in the concentration areas. The same was valid for the local bond (Fig. 5b). The addition of longer fibers (50 mm) slightly increased the bond stress. The average (middle) stress did not show many variations. The distribution of the radial bond stress component is presented in the Figure 6 for no fiber addition. The values for the radial stress (Fig. 6) were much lower compared to the shear stress with almost similar peak values, slightly higher with 50 mm (2 in.) of local bond.

Fiber addition in Figure 6b increased the stress values at the concentration points but not drastically as in the case of shear stress. The shear component was more critical at their concentration points and could develop to the bond breakdown. The size of the fibers did not make a big influence on the results.

3.4 *Cracks*

The experimental observations of the cracks in the concrete cylinder (Fig. 7 after Moradi 1994) after pulling of the rebar indicated the following. A cylinder made of plain concrete (Fig. 7a) was ruptured into three almost equal parts due to three radial splitting cracks. The fiber content (0.5%, 1% short fibers and 0.5% long fibers) in Figures 7b-d, retarded deformation in the load direction.

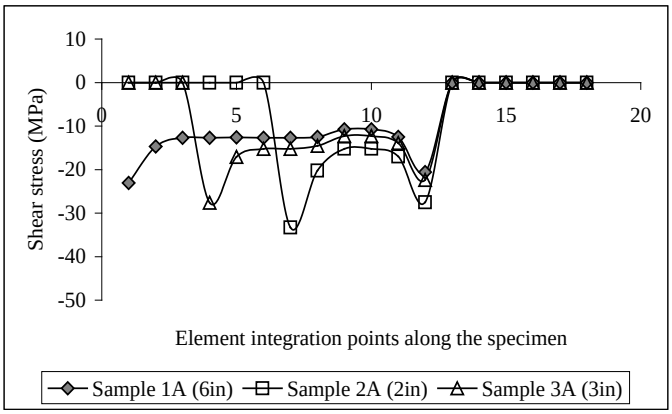

(a)

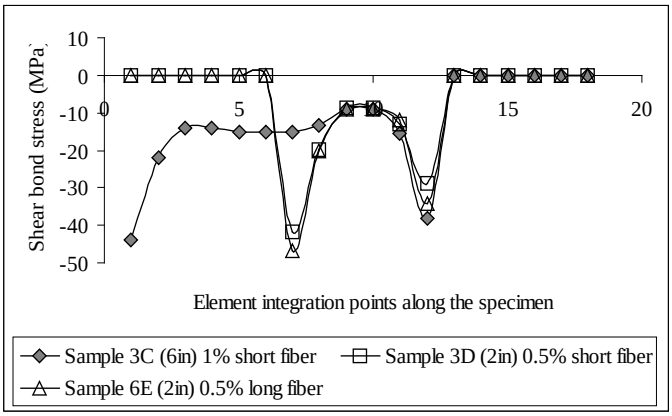

(b)

Figure 5. FEM results of shear stress along the specimen without fibers (a) and with short and long fibers (b).

Many radial cracks were visible on the surface but they did not cause splitting of the cylinder. The conclusion can be drawn that the addition of only 0.5% of synthetic fibers to the mix could improve the ductility and the energy dissipation capacity compared to the conventional plain concrete samples. The possible reason is that in FRC the fibers are closely spaced, which increases the efficiency in providing better crack control by improving the composite toughness.

In the finite element model, all samples showed identical initiation of cracks in the most softened concrete zone, in the bond zone while in the no bond zone only some symbolic cracking was noticed. The crack pattern was notified after the first 'load' step

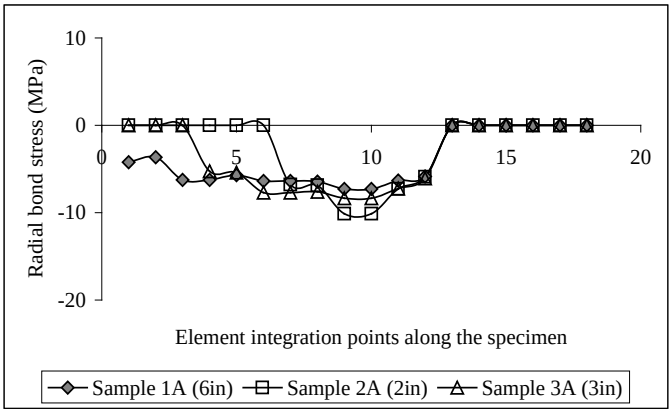

(a)

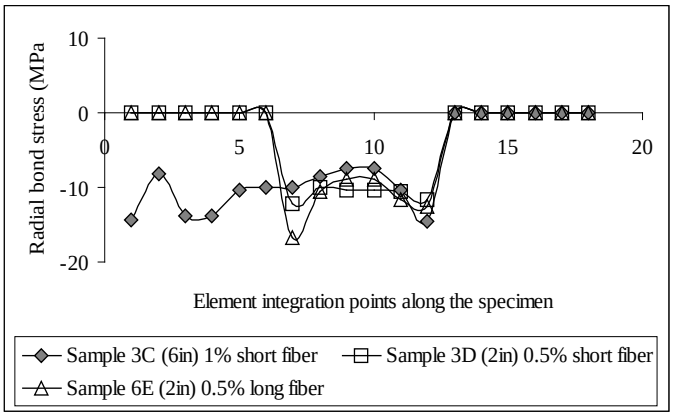

(b)

Figure 6. Radial stresses along the sample (a) without fibers and (b) with fibers.

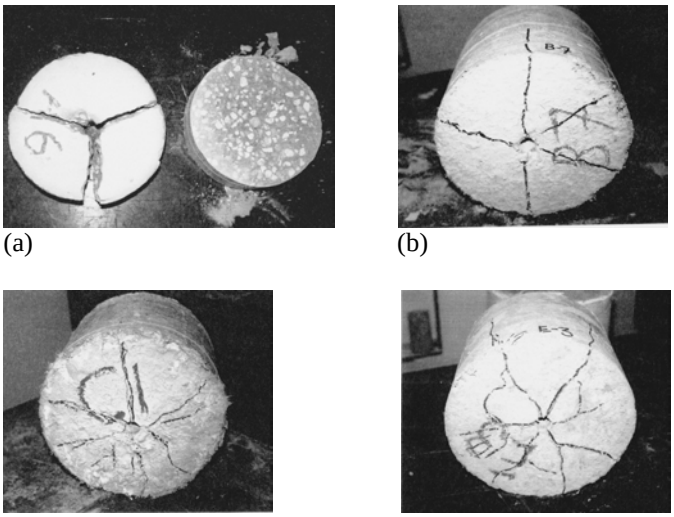

(a) (b)

(c) (d)

Figure 7. State of the specimens after the pull-out test (a) no fibers, (b) 0.5% short fibers, (c) 1% short fibers, (d) 0.5% long fibers (after Moradi 1994).

of 0.0025 mm in the numerical analysis (Fig. 8a). The first cracks were inclined and perpendicular to the maximum stress direction. As the slipping reached 0.4 mm (Fig. 8b), the crack pattern increased to a conical shape. Crack zones formed in the middle of the cylinder while the rest of concrete stayed uncracked. During the loading, cracks changed their status from 'open loading' (fully or partially) to the closed status. First occurred cracks in the vicinity of the rebar (interface bond zone)

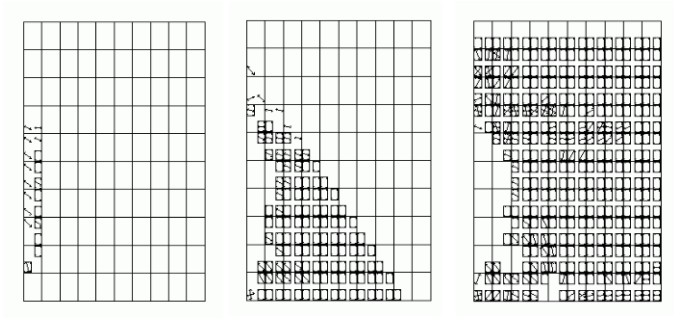

Figure 8. Cracking pattern of the plain cylinder after displacement of (a) 0.0025 mm, (b) 0.4 mm, (c) 3.5 mm.

were closed in the following load steps. The closing happened under a closing pressure such that cracks opened on one part of the specimen and closed on the other. Along with the inclined (shear) cracks, radial cracking occurred until the whole specimen was completely cracked (Fig. 8c). No experimental observations (microscopic or injection of ink, Goto 1971 etc.) were performed regarding the internal crack initiation. No exact conclusions can be drawn at this point. It might occur that the very first cracks developed due to the concrete drying shrinkage effect around the reinforcement before any load application.

4 DISCUSSION AND CONCLUSIONS

In order to model an interior joint in the reinforced concrete frame structures exposed to the seismic load, pull-out experiments and numerical analyses were performed on a one-sized cylindrical model. Non-linear finite element analysis was employed on a simple model to simulate experiments. The fracture mechanic approach was applied to study the bond mechanisms with material modelling of concrete, steel and interface zone. Fracture mechanics overcomes the drawbacks from the conventional methods: ultimate-limit analysis that considers only a single critical section for stress-strain analysis gives a different picture of the fracture process. Always present debonding and slipping of the steel-concrete in the interfacial zone in the vicinity of the cracked matrix can influence the service performance and the loading capacity of reinforced concrete structures but it is difficult to consider them in the conventional methods.

The bond-slip of the bar can be treated as independent of the concrete cover since the bar diameter was small compared to the cylinder diameter (d_c/d_b = 11) with the cover of 114 mm. This ratio was kept constant throughout the analysis. The effect of the fiber content on the bond stress including the decrease of the development length from the full bond 150 mm (6 in.) to the local bond of 50 mm and 75 mm (2 and 3 in.) was observed.

Decreasing of the development length from 150 mm (6 in.) to 50 and 75 mm (2 and 3 in.), decreased the load capacity but increased the bond stress. Results were also influenced by the fiber addition. Changes between 50 and 75 mm made a significant difference in shear and radial bond stress results. Local bond can be sufficient in the joints where smaller loading is expected. In that case, the bond stress will not be that easily broken.

Increasing of the percentage of fibers from 0% to 0.5 and 1%, the load capacity was increased when the full bond 150 mm (6 in.) was present. The displacements of the bar (slipping) at the peak load was not influenced by the fiber addition. The reason might be the insufficient fiber content, which did not develop sufficient strength support around the steel bar. On the other hand, the experimental mix design did not allow the increase of the fiber content. Possible changes in the mix design would be necessary to allow for more ductile concrete. Concrete was considered to be an elastically isotropic material before cracks occurred. Numerically, the crack origin was in the interface zone (bond elements). The explanation why cracks developed in the interface zone probably had to do with the different *E* (Young's modulus) of concrete and steel which 'confront' each other in the transition interface zone. The samples without fibers were completely cracked. The other samples with 0.5% and 1% were cracked on the surface but still kept the cylindrical shape. The cracks in radial direction occurred in plain concrete specimens while fiber reinforced cylinders cracked with mainly secondary cracking still keeping its cylindrical shape. Slipping of rebars along the cylinder increased with the increase of radial cracks, which was observed in both experiments and numerical 2-D analysis.

The stiffness of the bond elements was kept constant during the loading as well as other parameters, which is not the realistic situation. The reason was the limitations of the finite element analysis. That might be one of the reasons for the difference in the results between the finite element model and the experiments. Both results from the experiments and FEM must be taken with precaution since only monotonic load was modeled. Cyclic load (number of cycles) will probably show bigger differences in the results regarding the quality of the material (plain or fiber reinforced concrete).

The addition of fibers helped the increase of the fracture energy. By bridging the cracks, fibers prevented the applied stress to concentrate at the crack tip. Additional experimental trials could be made in the testing of a cylinder with the implementation of a smaller sized cylinder (in the bigger one) with higher fiber percentage in FRC around the rebar. Assuming a higher tensile and compressive strength of FRC, the higher resistance would be present in the mechanical interlock when chemical adhesion and friction are overruled. That could decrease crack propagation such that the rest of the cylinder could still be made of the plain concrete. The maximum value of the stress in this smaller cylinder member would depend on the elasticity of the fibers, the number of the fibers and possibly their inclination, depending on the fiber material. This could be applied in the numerical model. On the other hand, it is clear that the microcracking at the crack tip can be due to the ultimate strength collapse. As previously mentioned, the addition of fibers changed the structure of concrete. When fibers are added to the reinforced cementitious matrix, the interfaces that are formed between the fiber and matrix are significant

and can be helpful in determining the effective stress transfer between them. The further research of the fiber reinforced concrete will bring new results.

REFERENCES

Paulay, T., Park, R. & Priestley, M.J.N. 1978. Reinforced Concrete Beam-Column Joints under Seismic Actions. *ACI Journal, Proc.* Nov. 75 (11): 585-593.

Lutz, L.A. & Gergely, P. 1967. Mechanics of Bond and Slip of Deformed Bars in Concrete. *ACI Journal, Proc.* Nov. 64 (11): 711-721.

Mindess, S. 1989. Interfaces in Concrete. In J. Skalny (ed.), *Material Science of Concrete I*: 163-180. Westerville, OH: The American Ceramic Society, Inc.

Paulay, T. & Priestley, M.J.N. 1992. *Seismic Design of Reinforced Concrete and Masonry Buildings.* New York: John Wiley & Sons, Inc.

Abrams, D.A. 1913. Tests of Bond between Concrete and Steel, *Bulletin 71, Engineering Experiment Station*: 105. Urbana, IL. University of Illinois.

Brown, C.J., Darwin, D. & McCabe, S.L. 1993. Finite Element Fracture Analysis of Steel-Concrete Bond. *Structural Engineering and Engineering Materials, SM Report* 36, Lawrence, Kansas: University of Kansas Center for Research, Inc.

Tepfers, R. 1979. Cracking of Concrete along Anchored Deformed Reinforcing Bars. *Magazine of Concrete Research* 31: 3-12.

Reinhardt, H.W. & van der Veen, C. 1992. Splitting Failure of a Strain Softening Material due to Bond Stresses. In A. Carpinteri (ed.), *Application of Fracture Mechanics to Reinforced Concrete, Proc. Int. Workshop, Turin, Italy 1990*: 333-346. London: Elsevier Applied Science Publishers.

Goto, Y. 1971. Cracks Formed in Concrete around Deformed Tension Bars. *ACI Journal, Proc.* April 68 (4): 244-251.

Clark, A.P. 1946. Comparative Bond Efficiency of Deformed Concrete Reinforcing Bars. *ACI Journal, Proc.* Dec. 43 (4): 381-400.

Clark, A.P. 1949. Bond of Concrete Reinforcing Bars. *ACI Journal, Proc.* Nov. 46 (3): 161-184.

MacGregor, J.G. 1997. *Reinforced Concrete-Mechanics and Design*. Third Edition. New Jersey: Prentice Hall.

ACI Committee 544. 1982. State of the Art on Fiber Reinforced Concrete, *Concrete International* 4 (5): 9-25.

ACI Committee 544. 1994. Fiber Reinforced Concrete, Developments and Innovations. In J.I. Daniel & S.P. Shah (eds) *American Concrete Institute.* SP-142. Detroit.

Balaguru, P.N., Shah, S.P. 1992. *Fiber-Reinforced Cement Composites*. McGraw-Hill, Inc.

Bentur, A. & Mindess, S. 1990. *Fiber-Reinforced Cementitious Composites.* London & New York, Elsevier Applied Science.

Yin, W.S., Su, Eric C.M., Mansur, M.A. & Hsu, T. 1989. Biaxial Tests of Plain and Fiber Concrete, *ACI Materials Journal*, May-June 86 (3): 236-243.

Yin, W.S., Su, Eric C.M., Mansur, M.A. & Hsu, T. 1990. Fiber–Reinforced Concrete Under Biaxial Compression. *Engineering Fracture Mechanics* 35 (1/2/3): 261-268.

Soroushian, P., Mirza, F. & Alhozaimy, A. 1994. Bonding of Confined Steel Fiber Reinforced Concrete to deformed Bars. *ACI Journal* March-April 91 (2).

ACI-ASCE Committee 352. 1976. Recommendations for Design of Beam-Column Joints in Monolithic Reinforced Concrete Structures. *Journal of the American Concrete Institute* July, 73 (7): 375-393.

Moradi, M. 1994. Bond Characteristics of Polypropylene Fiber Reinforced Concrete. *M.S. Thesis, University of Central Florida.* USA, FL.

Jankovic, D. 1998. Numerical Modeling of Bond-Slip in Plain and Fiber Reinforced Concrete using Fracture Mechanics, *M.S. Thesis. University of Central Florida*. USA, FL.

TNO Building and Construction Research. 1996. DIANA, Finite Element Analysis, User's Manual, release 6.1, (eds) de Witte, F.C., Nauta, P.

Gijsbers, F.B.J., De Groot, A.K. & Kusters, G.M.A. 1978. A Numerical Model for Bond-Slip Problems: 37-48. IASS. Darmstadt.

De Groot, A.K., Kusters G.M.A. & Monnier Th. 1981. A Numerical Model for Bond-Slip Problems. *HERON* 26 (1B).

Nielsen, M.P., Braestrup, M.W. & Bach, F. 1978. Rational Analysis of Shear in Reinforced Concrete Beams, Int. *Assoc. Bridge and Structural Engineering, Proc*. May, P-15178.

Shah, S.P., Swartz, S.E. & Ouyang, C. 1995. *Fracture Mechanics of Concrete, Applications of Fracture Mechanics to Concrete, Rock, and Quasi-Brittle Materials*. New York: John Wiley & Sons, Inc.

Griffith, A.A. 1921. The Phenomena of Rupture and Flows in Solids. *Phil. Trans. Roy. Soc.*: 163-198. London, UK.

RILEM Draft Recommendations. Determination of the Fracture Energy of Mortar and Concrete by Means of Three-Point Bend Tests on Notched Beams. *Materials and Structures, Research and Testing*18 (106): 285-290.

Wittmann, F.H, Roelfstra, P.E., Mihashi, H., Huang, Y.Y., Zhang X.H. & Nomura, N. 1987. Influence of Age of Loading, Water-Cement Ratio and Rate of Loading on Fracture Energy of Concrete. *Materials and Structures* 20: 103-110. Paris: RILEM Publications.

Wittmann, F.H, Rokugo, K., Bruhwiler, E., Mihashi, H. & Simonin, P. 1988. *Materials and Structures.* 21 (21). Paris: RILEM Publications.

Reinhardt, H.W. 1989. Shear. In L. Elfgren (ed.) *RILEM: Fracture Mechanics of Concrete Structures; From Theory to Applications*. London: Chapman and Hall.

Different results are possible in the experimental specimens with the same material characteristics due to variability but not in the analytical modeling. Many factors influence an experiment, which can not always be measured and hence taken into account, while building numerical models. Beside other factors, the influence of the position of the bar during casting of concrete can be significant in the development of bond. The reason is the size distribution of the aggregates during casting. Even when the direction of casting and slip is identical, the bond stress and stiffness may only have 50% of the actual values if the slip is directed against the

casting direction (Dörr, 1978). In all experiments that were done by Moradi (1994), the casting and slipping were in the opposite directions.